Egypt. J. Chem. **Vol. 66**, No. 8. pp. 543 - 559 (2023)

Egyptian Journal of Chemistry

http://ejchem.journals.ekb.eg/

Theoretical and electrochemical studies of alkyl ammonium halide as impactful inhibitors for pipelines corrosion in oil well formation water

Mohamed A. Moselhy[1], Elsayed G. Zaki [2]*, Samir A. Abd El-Maksoud[3], Mohamed A. Migahed[2]

[1]Belayim Petroleum Company, 7074, Cairo, Egypt

[2]Egyptian petroleum Research Institute, Nasr City, Cairo (11727), Egypt

[3]Chemistry Department, Faculty of Science, Port Said University, Port Said 42522, Egypt

Abstract

To improve the resistance of carbon steel to corrosion in hostile settings, corrosion inhibitors are often applied to the steel. Both triethyl-hexyl-ammonium bromide (THAB) and dodecyl-triethyl-ammonium bromide (DTAB), which are cationic surfactants based on ammonium, were synthesized, described, and evaluated as potential corrosion inhibitors for API X-65 type steel in oil wells formation water under H2S conditions. Due to the fabrication of inhibitive film, the anti-corrosion properties of the carbon steel are significantly enhanced in the presence of organic corrosion inhibitors. In order to verify the THAB and DTAB chemical structures, a number of different spectroscopic methods such as FTIR and 1HNMR were utilized. Both potentiodynamic polarization and electrochemical impedance spectroscopy (EIS) measurements were utilized in this investigation to determine the effectiveness of the selected chemicals in inhibiting corrosion. The efficiency reached 81% for compound THAB and 82% for compound DTAB at 250 ppm It was revealed that the concentration of the inhibitor as well as the length of the spacer in their chemical structure both had an effect on the inhibition effect. Quantum chemical calculations and Monte Carlo simulation techniques were used to support the obtained experimental results.

Keywords: ammonium surfactants, EIS, Corrosion, Monte Carlo simulation, DFT

1. Introduction

The deterioration of metal is an inevitable process and is widely considered to be the biggest challenge that has a negative impact on the production rate since it directly affects industrial machinery across a variety of industrial contexts and applications, including the petroleum sector, power plants and cooling towers [1-6]. In most cases, traditional corrosion inhibitors are compounds that contain electronegative heteroatoms such as nitrogen, oxygen, sulphur, or phosphorus, unsaturated double bonds and aryl rings [7-11]. Surfactant inhibitors have many advantages such as high inhibition efficiency, easy production, low price, and low toxicity [12-15]. These compounds can coordinate with the metal atoms to form adsorbed layers on metal surfaces, which have the effect of preventing corrosion on metals [16-18]. It is possible for the metal's ability to resist corrosion to undergo a dramatic transformation as a result of the adsorption of the surfactant on its surface. Deep oil wells formation water that obviously occurs in the rocks before drilling contains a variety of dissolved inorganic and organic compounds. Formation water considers the most corrosive media in oil field procedures owing mainly to the presence of high amounts of the aggressive hydrogen sulfide, carbon dioxide and other corrosive salts such as sulfate and chloride [19]. In previous literatures, the mechanism of the corrosion process of carbon steel in various aqueous media containing H2S has been studied [20-25].The novelty is synthesis of novel amine compounds with high efficiency to corrosion mitigate

The present work is aimed to synthesis of two novel cationic surfactants namely; (THAB and DTAB) and evaluation of their performance as

*Corresponding author e-mail: chemparadise17@yahoo.com.; (ELSAYED G. ZAKI).
Received date 28 September 2022; revised date 11 November 2022; accepted date 20 November 2022
DOI: 10.21608/ejchem.2022.165887.7043

corrosion inhibitors for carbon steel in oil wells formation water under H2S environment by using different techniques. Adsorption isotherm was utilized to elucidate inhibitors interaction with metal surface. Theoretical studies were used to support the obtained experimental data.

2. Experimental section

2.1. Chemical composition of API 5L -X65 type carbon steel alloy

Carbon steel specimens used in this investigation were cut from unused petroleum pipeline (Belayim Petroleum Company - Egypt). The chemical composition (weight %) of carbon steel was as follows: C (0.09), Si (0.22), Mn (1.52), P (0.01), S (0.05), Ni (0.04), Cr (0.02), Mo (0.004), V (0.002), Cu (0.02), Al (0.04) and Fe (97.984).

2.2. Synthesis of the inhibitors

The cationic surfactant (DTAB and THAB) based on tri-n-ethyl amine was synthesized by quaternization reaction as outlined in Scheme 1. Tri-n-ethyl amine at a concentration of 50 mM and 1-bromododecane or 1-bromohexane at the same level were each put into a round flask of 250 mL containing (CH3)2CO at a volume of 100 mL as a dissolvable solvent [26]. The final blend was brought down to room temperature after undergoing an 18-hour mixing process during which it was subjected to a reflux heating method. After being filtered via filter paper, the earthy colored suspension was rinsed well twice with diethyl ether and then recrystallized from (CH3)2CO in order to cover the expense of the white gem that the cationic surfactants produced. The outputs of the earthy colored precious stone items ranged anywhere from 80–90% in terms of their total product value.

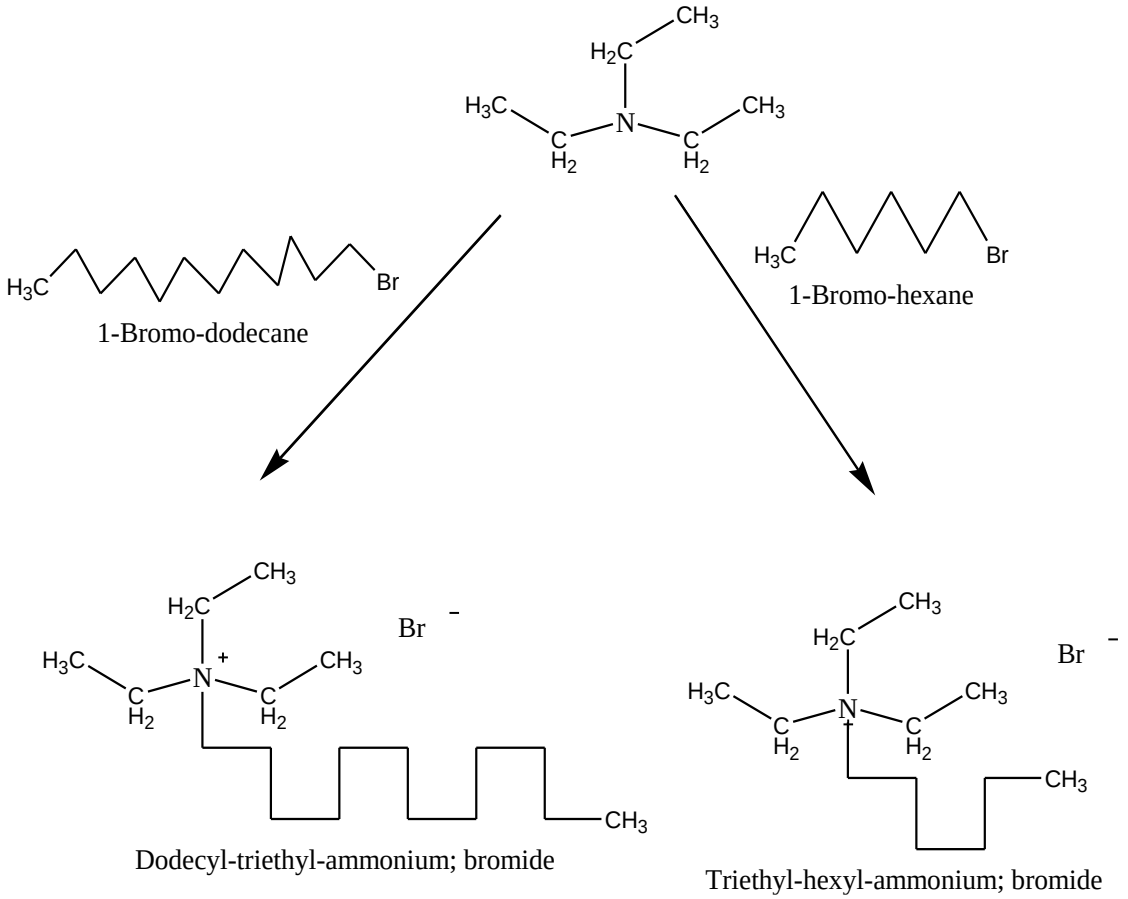

Scheme 1: Synthesis of cationic surfactant (THAB, DTAB)

2.3. Solution

The corrosive solution utilized in this study is deep oil well produced water obtained from Belayiem Petroleum Company (Petrobel) – Egypt. Chemical composition and physical properties of deep oil well produced water used in this work were listed in Table 1. The test solution for this study contains reaction of sodium sulfide (3.53 mg/L) with acetic acid (1.7 mg/L) to produce H2S gas.

Table 1: Chemical composition and physical properties of deep oil well formation water used in this investigation

Physical properties		
Property	**Unit**	**Value**
Density	g/mL	**1.06**
T.D.S	mg/L	**9650**
pH at 25 ºC		**6.8**
Specific gravity		**1.06**
Salinity (as NaCl)	ppm (mg/l)	**95556**
Total alkalinity (as $CaCO_3$)	Ppm	**320**
Total hardness (as $CaCO_3$)	Ppm	**14455**
Resistivity	Ohm-m @21.6 ºC	**0.0832**
Conductivity	mhos/cm@21.6 °C	**12.02** x **10^{-2}**
Chemical properties		
Ionic species	**mg/L**	**meq/L**
Lithium	48.9	7.056
Sodium	30760.9	1337.485
Potassium	945.24	24.179
Calcium	4225.67	210.861
Magnesium	947.95	78.007
Barium	1.30	0.019
Strontium	78.08	1.783
Iron	Nil	Nil
Copper	Nil	Nil
Fluoride	76.71	4.038
Chloride	57912.87	1631.405
Bromide	252.62	3.163
Ammonium	186.85	10.357
Carbonate	Nil	Nil
Bicarbonate	390.40	6.399
Phosphate	Nil	Nil
Sulfate	640.54	13.342
Sulfide	325	0.020
Nitrite	1.84	0.040
Nitrate	38.17	0.616

2.4. Corrosion measurements

Electrochemical studies (PDP and EIS) were performed by a three-electrode electrochemical glass cell using Volta lab 80 potentiostat (Tacussel-Radiometer PGZ−402). Volta lab 80 was controlled by Tacussel corrosion analysis software model (Volta master 4). API 5L X65 carbon steel with an exposed surface area of 1 cm2 was used as the working electrode, platinum plate was served as the counter electrode, and saturated calomel electrode (SCE) was employed as reference electrode. Before starting the measurements, the working electrode was polished in series on 360-2500 silicon carbide papers, then rinsed with deionized water and acetone, and finally dried under warm air. PDP tests were performed at ± 300 mV based on EOCP with a constant sweep rate of 1 mV s−1 [27, 14]. The corrosion potential and the corrosion current density were collected by extrapolation at Tafel segments of the obtained anodic and cathodic polarization curves. EIS experiments were carried out at open circuit potential (EOCP) in a frequency range between 100 kHz and 0.02 Hz, with a signal (AC) amplitude perturbation of 10 mV [28, 29]. After the measurements, the EIS data obtained were interpreted by ZSimpwin software. EIS diagrams are given in both Nyquist and Bode plots. Each electrochemical test had been carried out at least twice to confirm the accuracy of the data.

2.5. Computational Calculations

In the course of this research, the software known as Gaussian 09 W was utilized to do quantum chemical calculations. At the level of the DFT calculation, a neutral and cationic LP (LP, LPH+) +G(d, p) basis set is used. Following the acquisition of the corresponding quantum chemical parameters, a detailed discussion took place. To understand the metal's inhibitive performance, it is essential to conduct research on the adsorption mechanism of inhibitor molecules on the surface of the metal and the corresponding bonding strength of these molecules. Using the molecular mechanics method, which was implemented in the Forcite module, we were able to emphasize the contact that occurred between the inhibitor molecules and the steel surface. It was decided to construct a simulation box with dimensions of 24.3 17.2 67.1 A. This box would have 5 layers of Fe (110), 1 inhibitor molecule, 500 H2O molecules, and a 40 A vacuum layer. In this particular system, the periodic boundary condition and the COMPASS force field were implemented. With a simulation period of 500 ps and a time step of 1 fs, employing the NVT canonical ensemble was successful in producing a simulation of high quality [30-33].

3. Results and discussion

3.1. FTIR spectroscopic analysis

FTIR spectrum (Figure 1) of the prepared inhibitors (DTAB, THAB) shows two peaks at 3355 cm−1 and 3410 cm−1 are ascribed for N-H in both inhibitors, 2925 and 2856 cm−1 corresponding to (CH3 and CH2), in addition to peak at 1059 cm−1 and fingerprint peak at 724 cm−1 referred to the asymmetric and symmetric stretching quaternary nitrogen atom (N+─C) as shown in Scheme 1.

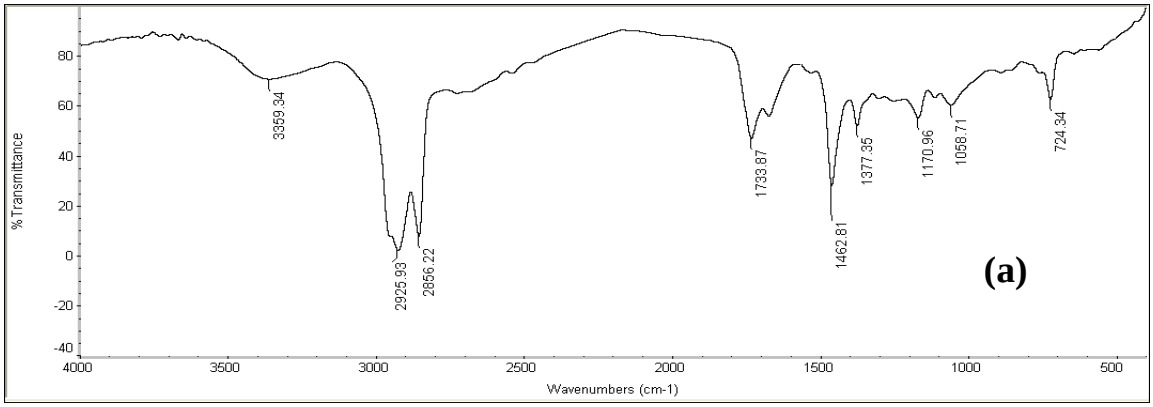

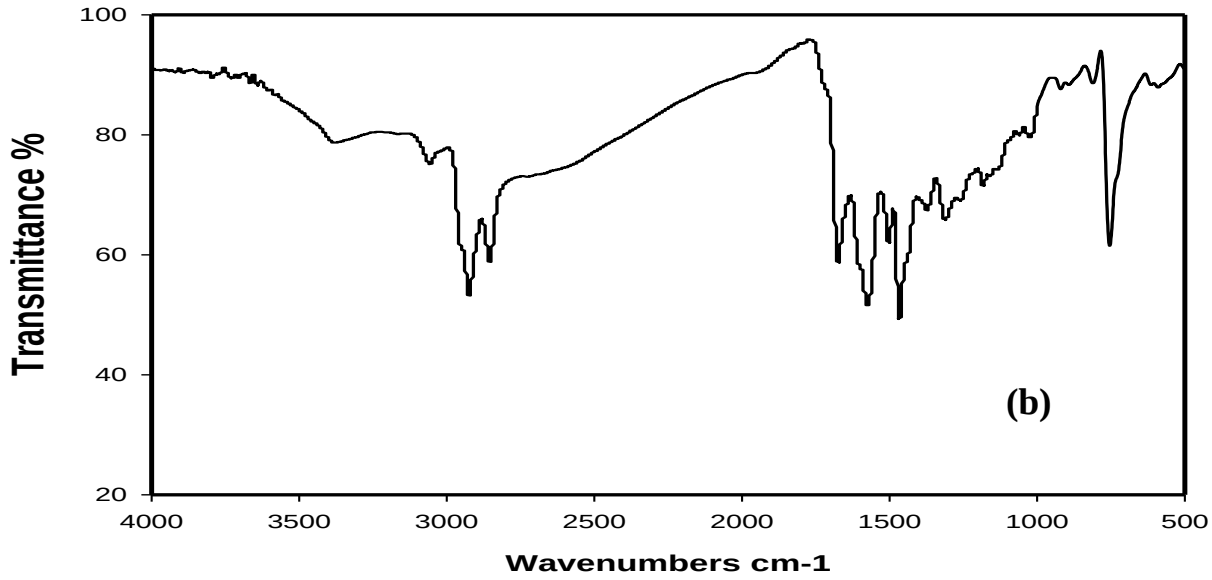

Figure 1(a, b): FTIR spectrum of the synthesized inhibitors: (a) DTAB and (b) HTAB.

3.2. ^{1}H NMR spectrum spectroscopic analysis

Figure 2 (a, b) show the chemical shift at ϭ (0.96) for 1H proton (a) –CH3, the chemical shift ϭ (3.33), (1.73) for 1H protons attached to nitrogen atoms (b) and . All the above chemical shifts confirm that compound DTAB was successfully prepared. The above chemical shifts confirm that THAB were successfully prepared. The data of 1H NMR spectra confirmed the expected hydrogen proton distribution in the synthesized surfactant as shown in Figure 2(a, b).

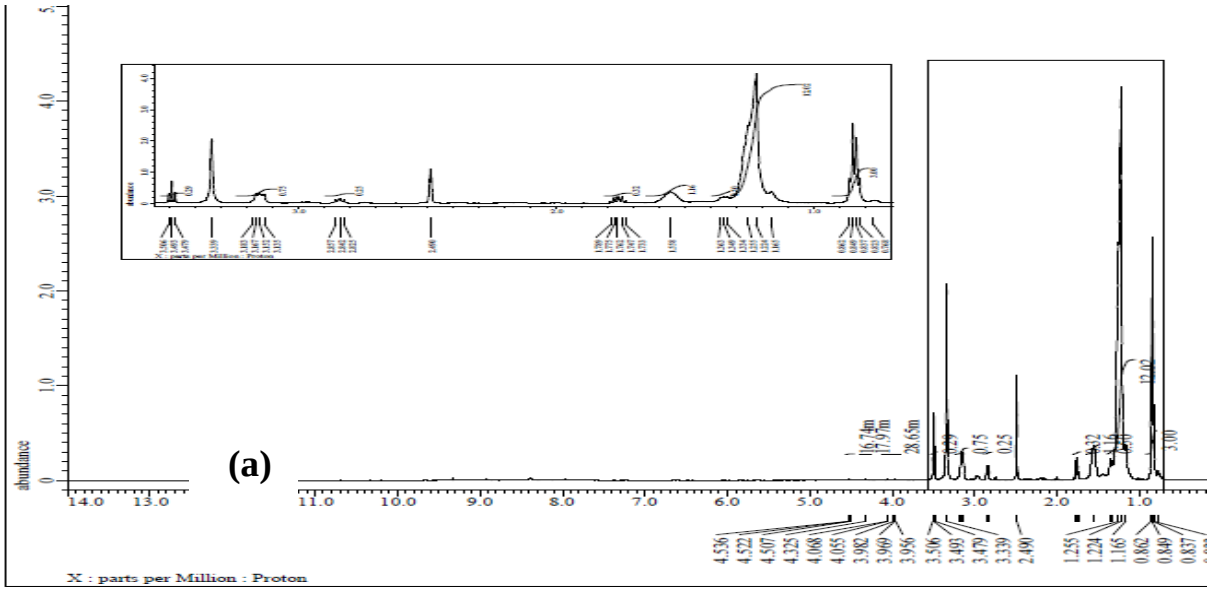

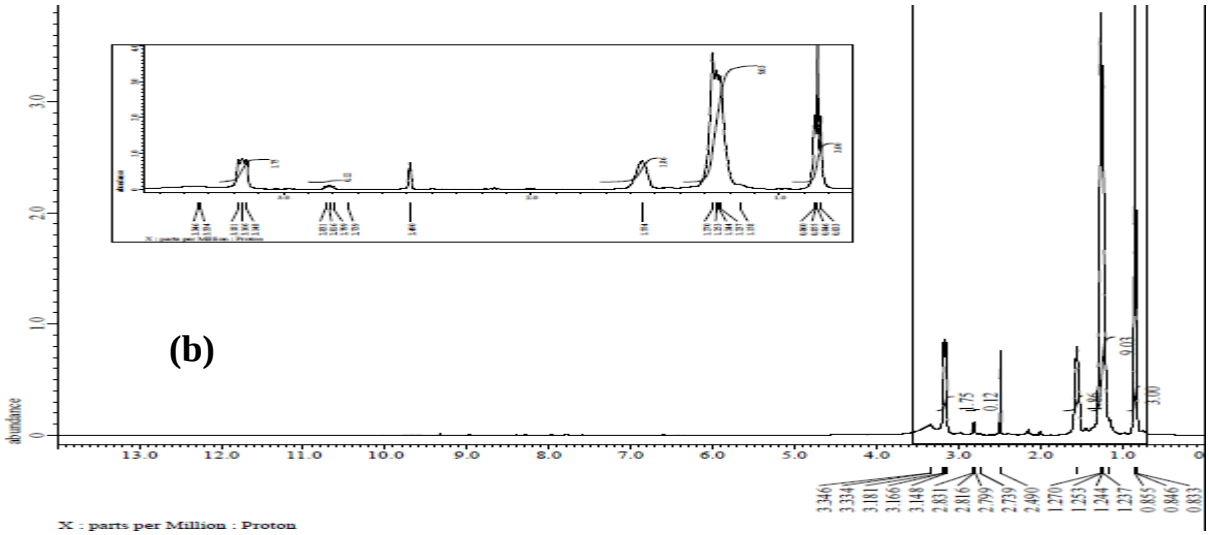

Figure 2: Chemical structure characterization of inhibitor, (a) 1H-NMR DTAB and (b) 1H-NMR HTAB

3.3. Potentiodynamic polarization measurements

The anodic and cathodic polarization curves for carbon steel in formation water without and with various concentrations of inhibitors are shown in Figure 3. Calculations were made to determine electrochemical parameters such as corrosion potential (Ecorr.), corrosion current density (icorr.), cathodic and anodic Tafel slopes (βc and βa), and polarization resistance (Rp). Complete data obtained from potentiodynamic polarization measurements are summarized and listed in Table 2. It is obvious from Table 2 that the corrosion current density significantly decreased in the presence of the investigated inhibitors compared to uninhibited solution, indicating that two compounds (THAB and DTAB) retarded the corrosion of carbon steel in formation water [34, 35].

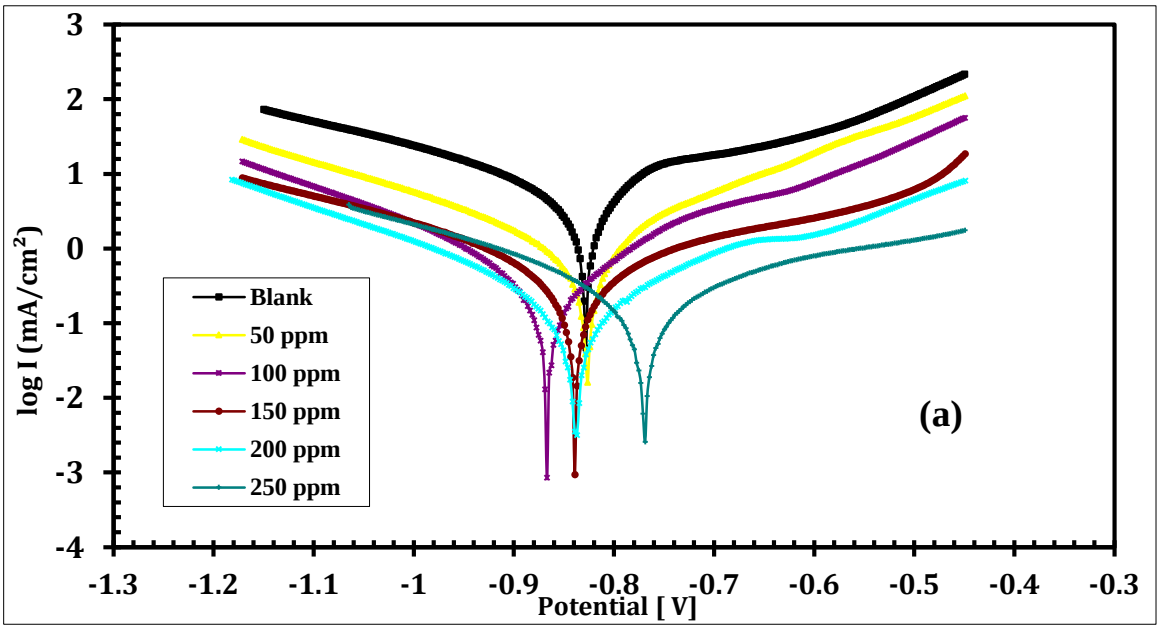

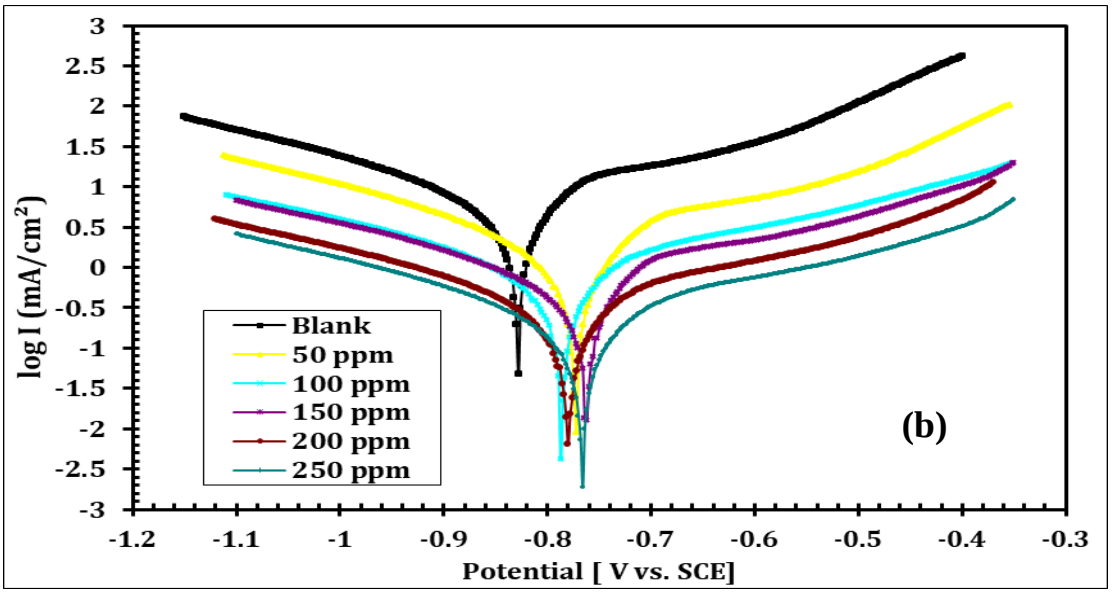

Figure 3: Polarization plots of steel electrode attained in formation water and containing various concentrations of (a) THAB and (b) DTAB inhibitors.

The degree of surface coverage (θ) and the percentage inhibition efficiency (η %) were calculated using the following equations **[36-38]** :

$$\eta_{PDP} = \boldsymbol{\theta} \times 100 = \left[\frac{i^0_{corr} - i_{corr}}{i^0_{corr}}\right] \times 100 \qquad (1)$$

Where i^0_{corr} and i_{corr} are the corrosion current densities in the absence and presence of the inhibitor, respectively. A careful inspection of the polarization curves indicated that Tafel lines are shifted to more negative and more positive potentials for the anodic and cathodic processes, respectively relative to the blank curve. This means that the selected compounds acts as mixed type inhibitor and the corrosion current densities (i_{corr}) are decreased with increasing concentration. The data in **Table 2** revealed that the inhibition efficiency obtained using the I_{corr} values increase with the increasing of the inhibitor concentrations. The results indicate that the percentage inhibition efficiency (η %) of compound (DTAB) is greater than that of compound (THAB). This could be attributed to the long alkyl chain of the DTAB inhibitor, and this could be attributed to the increase which leads to an increase in the surface area of each molecule covering the surface of carbon steel and isolating it from the aggressive environment **[39, 40]**.

Table 2: Corrosion parameters obtained from polarization curves for THAB and DTAB inhibitors.

Inhibitor	Conc. (ppm)	β_a mV/dec	$-\beta_c$ mV/dec	$-E_{corr}$ mV vs. SCE	I_{corr} µA/cm²	Θ	Η %
Blank	---	193.7±2	150.9±3	825±4	9.312±0.1	----	----
THAB	**50**	126.5±1	152.4±3	805±1	3.514±3	0.6108±0.5	61.08
	100	131.7±2	141.3±2	801±3	3.238±2	0.6421±0.2	64.21
	150	107.8±3	136.5±1	798±2	2.305±1	0.7534±0.3	75.34
	200	105.2±1	129.2±3	792±4	2.142±3	0.7812±0.1	78.12
	250	101.4±2	122.7±4	780±1	1.697±2	0.8105±0.4	81.05
DTAB	**50**	129.4±3	158.2±1	818±3	3.435±0.2	0.6313±0.05	63.13

	100	133.8±1	145.3±1	833±2	3.092±0.1	0.6680±0.01	66.8
	150	108.5±2	128.6±2	809±1	2.054±0.3	0.7795±0.04	77.95
	200	106.1±1	123.8±4	803±2	1.939±0.4	0.7918±0.03	79.18
	250	103.6±4	117.4±2	785±4	1.598±0.2	0.8284±0.02	82.84

3.4. Electrochemical impedance spectroscopy (EIS) studies

The corrosion inhibition of carbon steel in oil wells formation water in the absence and presence of different doses of compounds (THAB and DTAB) was performed using EIS method. **Figures 4, 5** show the Nyquist plots for THAB and DTAB inhibitors. It is clear from Nyquist plots that there is a depressed capacitive loop along the X-axis and the size of loop increased by increasing the inhibitor concentration, indicating the adsorption barrier layers of these compounds (THAB and DTAB) formed on carbon steel in corrosive solution, preventing the dissolution of iron in oil well formation water **[41-44]**. The concentration of the inhibitors does not change the shape of the EIS figure, indicating that these inhibitors control the corrosion reaction activity rather than alter the corrosion mechanism **[45, 46]**. The electrical equivalent circuit as shown in **Figure 6** has been precisely proposed to fit the impedance measurements consisting of the solution resistance (Rs), the charge transfer resistance(R_{ct}) and the double-layer capacity (C_{dl}). The impedance parameters were listed in **Table 3**. The inhibition efficency (η%) and surface coaverge (θ) of the surfactant inhibitors were listed in **Table 3** and estimated by thefollowing expression **[47, 48]**:

$$\eta_{EIS}\% = \theta \times 100 = \left(1 - \frac{R_{ct}}{R_{ct(inh)}}\right) \times 100 \quad (2)$$

Where, $R_{ct(inh)}$ and R_{ct} are the values of the charge transfer resistance in the absence and present of the inhibitors, respectively.

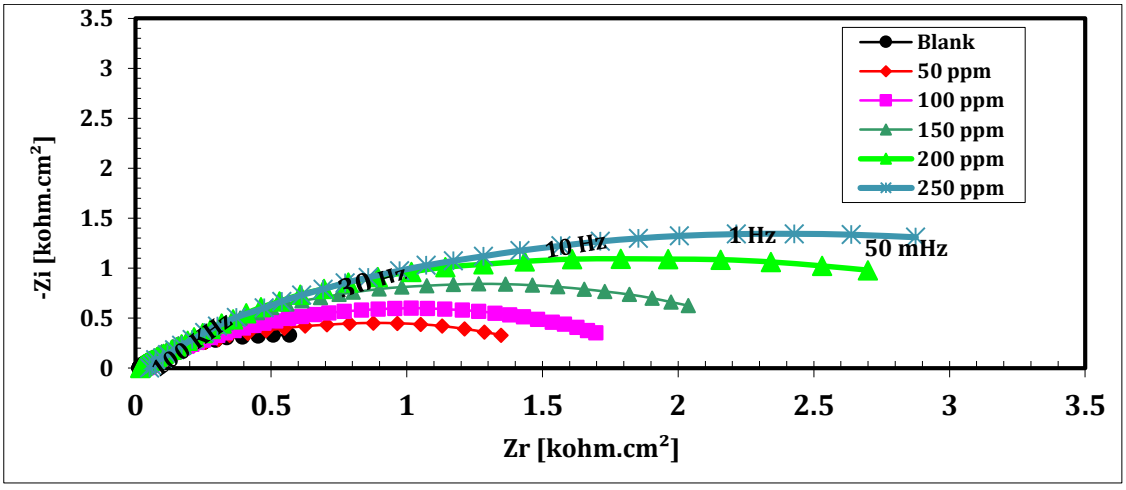

Figure 4: Nyquist plots for carbon steel electrode in formation water with and without various concentrations of THAB inhibitor

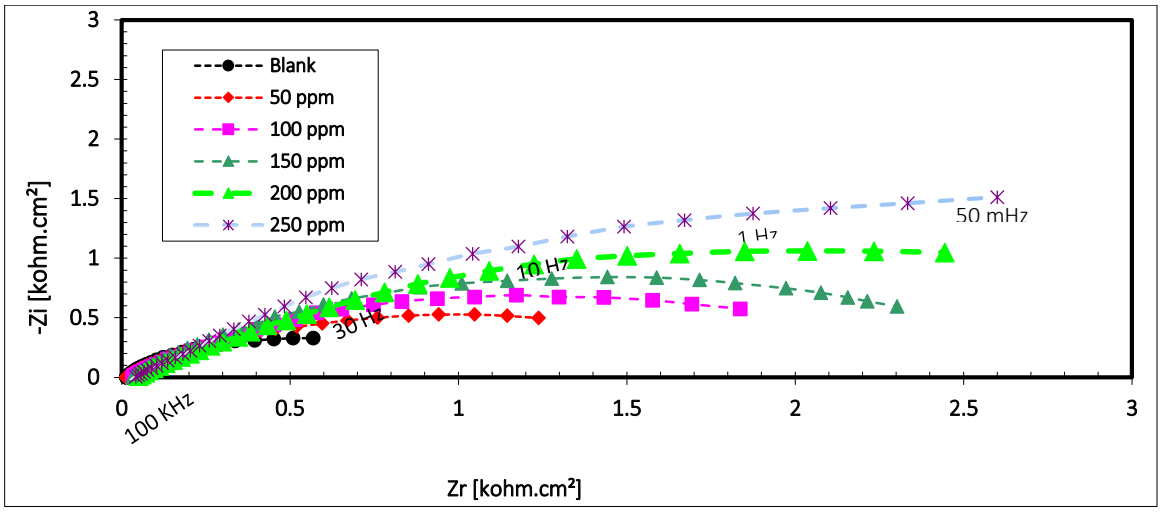

Figure 5: Nyquist plots for carbon steel electrode in formation water with and without various concentrations DTAB inhibitors.

Table 3: Impedance parameters obtained from EIS curves for **THAB** and **DTAB** inhibitors.

Inhibitor	Conc. (ppm)	R_f Ω	Q_f µf/cm²	n_1	Q_{dl} µf/cm²	R_{ct} KΩ/cm²	n_2	Θ	IE%
Blank	---	48.3±2	132.1±1.1	0.87±0.02	538.1±7	1.659±0.1	0.83±0.05	-----	----
THAB	50	111.7±3	71.3±0.9	0.87±0.03	237.2±6	4.187±0.2	0.87±0.04	0.6038	60.38
	100	173.2±5	52.8±0.8	0.88±0.01	184.3±5	4.534±0.3	0.90±0.03	0.6341	63.41
	150	215.6±4	41.3±0.7	0.89±0.01	135.9±4	6.002±0.4	0.91±0.02	0.7236	72.36
	200	287.3±6	35.7±0.6	0.90±0.02	113.7±3	7.071±0.5	0.91±0.03	0.7654	76.54
	250	305.2±5	22.1±0.5	0.91±0.01	109.8±2	8.690±0.6	0.92±0.01	0.8091	80.91
DTAB	50	115.3±3	73.8±0.9	0.87±0.04	243.8±5	4.401±0.2	0.88±0.02	0.6231	62.31
	100	183.1±5	54.6±0.8	0.88±0.01	198.4±3	4.767±0.3	0.91±0.03	0.6527	65.27
	150	233.7±4	44.2±0.7	0.89±0.03	138.2±2	6.716±0.4	0.93±0.04	0.7528	75.28
	200	297.4±6	37.3±0.6	0.90±0.02	117.9±2	7.222±0.5	0.94±0.02	0.7703	77.03
	250	313.7±7	24.7±0.5	0.91±0.01	111.5±4	9.11±0.6	0.95±0.02	0.8180	81.80

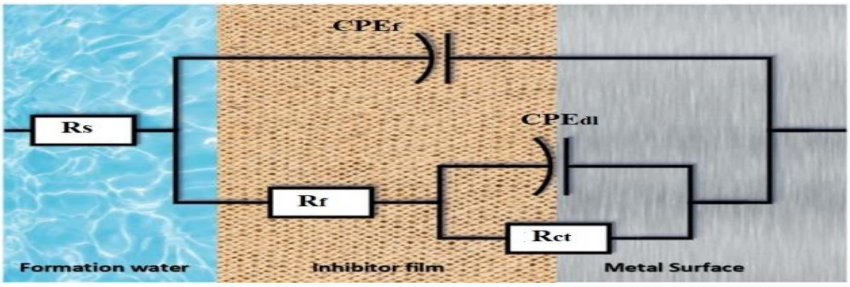

Figure 6: Equivalent circuit used to model impedance data of carbon steel in oil well formation water under H_2S environment.

It is obviously from **Table 3** that the R_{ct} value and $\eta_{EIS}\%$ value increase with increasing concentration of THAB and DTAB inhibitors. Moreover, both C_{dl} value and C_f value decrease with increasing concentration of THAB and DTAB inhibitors. This indicates that the increase in the thickness of the protective layer was formed on carbon steel in deep oil wells formation water solution. According to the next two equations **[24]**:

$$C_{dl} = \sum^{0}\sum Se/d \quad (3)$$

$$C_f = F^2Se/4RT \quad (4)$$

Where d is the thickness of the adsorbed layer, Se is the electrode surface exposed to the aggressive solution, $\sum^0$ is the permittivity of the vacuum, $\sum$ is the local dielectric constant and F is the Faradays constant. C_{dl} value was reduced upon raising the dose of inhibitors. This can be explained by replacing the water molecules with adsorption of the studied inhibitor molecules that create protective layers on the surface of carbon steel electrode and blocks corrosion reactions on carbon steel surface **[49]**. Bode plots revealed that the phase angle increased with increasing dose of these (THAB and DTAB) inhibitors for carbon steel in formation water compared to the blank solution. Also, the variation of log Z with log F revealed that the impedance values increase with increasing concentration. The higher inhibition efficacy could be due to the presence of N atoms and the use of a surfactant with a larger alkyl chain length that provides strong adsorption centres and increases the layer thickness **[50]**.The inhibition efficiency gradually increases with increasing the alkyl chain length of the prepared compounds (as shown in **Table 4**, and the order of inhibition efficiency was in the following order: DTAB > THAB, which is in consistent with the obtained potentiodynamic polarization results.

3.5. Molecular modeling

The produced surfactants have a high adsorption propensity over the Carbon steel surface. This is because the chemical structure of the surfactant has a high number of function groups that are rich in electrons. The DFT method can demonstrate how the electron density is distributed across the atomic and molecular structures of substances. The DFT output parameters are the major indices that are used in the calculation of the other parameters according to the equations. These indices are as follows: the energy of the highest full-field molecular orbital (E_H), the energy of the lowest empty molecular orbital (E_E), and the total energy of the molecular orbitals (E_L)

$$\Delta E_{gap} = E_L - E_H \quad (5)$$

$$\eta = \frac{\Delta E_{gap}}{2} \quad (6)$$

$$\sigma = \frac{1}{\eta} \quad (7)$$

The work function of the 110th planar configuration of iron is 4.82 eV (Fe). It has been determined that the donor-acceptor interaction between THAB and DTAB, in addition to the 3-dimensional orbital of iron, is responsible for promoting adsorption. The donation of electrons from THAB and DTAB into the empty 3-dimensional iron orbital is facilitated by an increase in the values of EH .DTAB and THAB are better equipped than EL to acquire electrons from full-field, three-dimensional iron orbitals. The electron cloud in the solution phase is distributed over imine-azo dye, hetero and aromatic moieties (pyridine, phenol), and halogenated groups **[48, 51]**. This is seen in **Figure 7**. The electron density for HOMO in the gas phase is distributed over quaternary nitrogen and halogen atoms. In both the gaseous and the solvated phases, LUMO electrons are found to be spread over the identical HOMO centers **[52, 53]**. It is believed that both Homos and Lumo are centers of interaction between donors and acceptors. An electrostatic potential map that illustrates the dispersion of electron clouds is used in **Figure 7** to illustrate both alkyl chains and the alkyl chains. This reveals that both THAB and DTAB have tendency to generate an adsorption film more denser and more adhesive than other films.

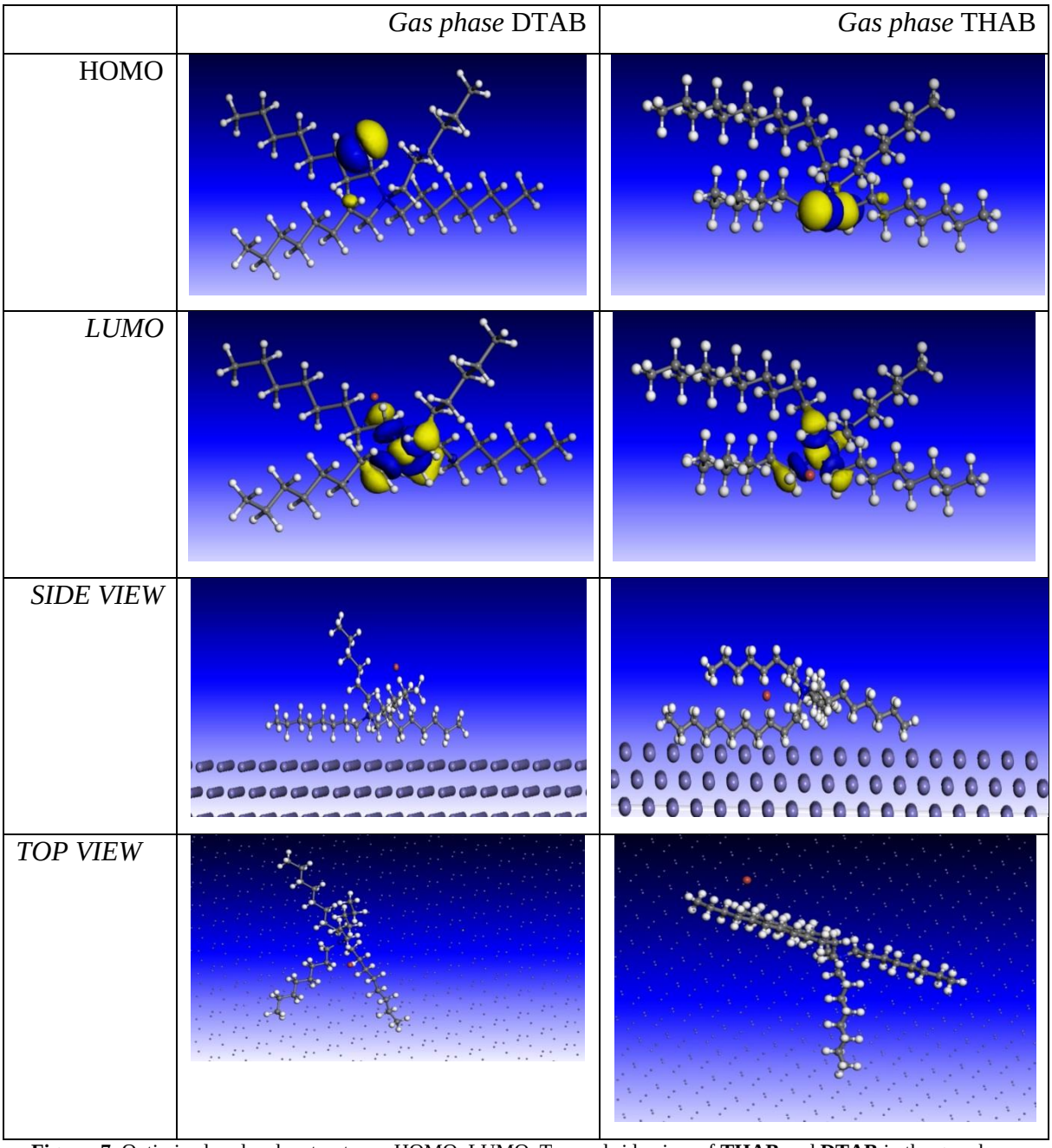

Figure. 7. Optimized molecular structures, HOMO, LUMO, Top and side view of **THAB** and **DTAB** in the gas phase.

THAB and DTAB are electron donors that transport electrons from one metal surface to another metal surface. The values for N in the gas phase are shown to be less than 3.6 in **Table 4**. The back-donation energy, denoted by the symbol Eback-donat, may be found in **Table 4**. This energy shows that electrons from full-filled 3-d or 4S orbitals of Fe are donated to the LUMO of DTAB and THAB. The compound adsorption activity has been confirmed by both the donation and back-donation techniques.

Table 4: Quantum chemical parameters of the investigated inhibitors

Parameters	E_H (ev)	E_L (ev)	ΔE_{gap}	A	I	X	η	ΔN
THAB	-7.989	-0.514	7.475	0.514	7.989	4.2515	3.7375	0.367692308
DTAB	-8.517	-0.113	8.404	0.113	8.517	4.315	4.202	0.319490719

3.6. Monte Carlo simulation (MCS)

In these images (**Figure. 7**), the molecules of DTAB and THAB are arranged in a fashion that is most suited to the plan of the Fe crystals that is known to be the most stable (110). It is possible to simulate the adsorption properties of components DTAB and THAB on CS surface alloy by using the MCs procedure. The adsorption process (donor-acceptor interactions) is carried out effectively, as indicated in the side and top views of **Figure. 7**, as a result of the flat and planer orientation positions of the DTAB and THAB optimized structure in gas and solvent phases over Fe (110). DTAB and THAB have a substantial spontaneous adsorption affinity over the CS alloy surface, as shown by the data in Table 6, which results in large negative values of adsorption energy (E_{ads}) in gas or solvated phases. It is important to take into consideration the fact that the value of $_{Eads.}$ In the solvent phase is higher than the comparable value in the gas phase. This is because of the creation of H-bonds between the molecules of the water solvent and the nitrogen or/and oxygen atoms of DTAB and THAB. These H-bonds act in a synergistic manner to adsorb DTAB and THAB to the surface of the CS. This is because the. Value of E_{ads} for (DTAB and THAB) is higher than its value for water, which explains why we have this result. It has been demonstrated that components DTAB and THAB are capable of producing a protective adsorption barrier film on the surface of component CS alloy. The interpretations of the DFT and MCs output indices are consistent with the gravimetric and electrochemical data obtained from the laboratory.

DTAB and THAB exhibit a strong spontaneous adsorption affinity over the CS surface, as shown by the data in **Table 5**, which results in substantial negative values of adsorption energy (E_{ads}) in gas or solvated phases. This is the case whether or not the CS is in a gas or solvated phase. It is important to take into consideration the fact that the value of Eads. in the solvent phase is higher than the comparable value in the gas phase. DTAB adsorption on the surface of the CS is made easier as a result of the H-bond that is created between the molecules of the water solvent and the nitrogen or/and oxygen atoms in the chemical **[54-61]**. This reveals that chemicals are capable of substituting water molecules that are adsorbing onto the surface of the CS and producing a protective adsorption barrier coating.

Table 5: The outputs energies calculated by Monte Carlo simulation for DTAB and THAB in gas phase on Fe (110)

Parameters	Total energy	Adsorption energy	Rigid adsorption energy	Deformation energy	3D Atomistic
DTAB	-345.021705	-426.3217956	-238.7488623	-187.5729334	-426.32
THAB	-411.09547	-539.5453442	-277.6503083	-261.8950359	-539.55

Comparison between the advantages and economics of the presented study and previous work are listed at table 6

Table 6. Comparison between advantages and economics of the present study and previous works.

Compounds	**Media**	**Type**	**Efficiency %**	
TEAEMO triethanolamine ester of MO adduct	1 M H_2SO_4	Surfactants	63	**[62]**
quinine, ephedrine, brucine, cinchonine, codeine, and harmaline	2M H2SO4	aromatic rings	74	**[63]**
triethyl-hexyl-ammonium bromide (THAB) and dodecyl-triethyl-ammonium bromide (DTAB(	oil well formation water	Surfactants	82	Current work

4. Conclusions

The newly synthesized surfactants THAB and DTAB have the potential to be efficient inhibitors for the dissolving of carbon steel in the water found in deep oil well formations. FTIR and nuclear magnetic resonance (1HNMR) spectroscopy techniques were utilized so that the structure of the surfactants could be examined and validated. The polarization data that were collected provided conclusive evidence that the cationic surfactants of choice function as mixed-type inhibitors. The inhibition efficiency reaches 82 % for the optimum concentration of the THAB and DTAB inhibitors. In conclusion, the Monte Carlo simulation method served to validate the hypothesis that there is a correlation between the experimental and theoretical findings.

5. Conflicts of interest

The authors declare no competing interests.

6. Formatting of funding sources

There is no fund

7. Acknowledgments

The authors would like to thank the Egyptian Petroleum Research Institute (EPRI) for their help and collaboration in completing this work

8. References

[1] P. R. Roberge, Corrosion engineering, *McGraw-Hill Education*, 2008.

[2] N. E. Basiony, A. Elgendy, H. Nady, M. A. Migahed, E. G. Zaki, Adsorption characteristics and inhibition effect of two Schiff base compounds on corrosion of mild steel in 0.5 M HCl solution: experimental, DFT studies, and Monte Carlo simulation, *RSC advances*, **9**(2019) 10473-10485.

[3] M. Finšgar, J. Jackson, Application of corrosion inhibitors for steels in acidic media for the oil and gas industry: A review, *Corrosion Science*, **86** (2014) 17–41.

[4] M. A. Migahed, E. G. Zaki, M. M. Shaban, Corrosion control in the tubing steel of oil wells during matrix acidizing operations**,** *RSC Advances*, **6** (2016) 71384–71396.

[5] M. M. Solomon, S. A. Umoren, M. A. Quraishi, M. Salman, Myristic acid based imidazoline derivative as effective corrosion inhibitor for steel in 15% HCl medium, *Journal of Colloid and Interface Science*, **551** (2019) 47–60

[6] M. A. El-Monem, M. M. Shaban**,** M. A. Migahed, and M. M. H. Khalil**,** Synthesis, Characterization, and Computational Chemical Study of Aliphatic Tricationic Surfactants as Corrosion Inhibitors for Metallic Equipment in Oil Fields**,** *ACS Omega*, **5** (2020) 26626–26639

[7] A. Singh, K. Ansari, M. Quraishi, H. Lgaz, Y. Lin, Synthesis and investigation of pyran derivatives as acidizing corrosion inhibitors for N80 steel in hydrochloric acid: Theoretical and experimental approaches, *Journal of Alloys and Compounds*, **762** (2018) 347–362.

[8] M. A. Migahed, M. M. El-Rabiei, H. Nady, E. G. Zaki, Novel Gemini cationic surfactants as anti-corrosion for X-65 steel dissolution in oilfield produced water under sweet conditions: Combined experimental and computational investigations. *Journal of Molecular Structure*, **1159**(2018)10-22.

[9] M. A. Bedair, S. A. Soliman, M. F. Bakr, E. S. Gad, H. Lgaz, I. M. Chung, & F. Z. Alqahtany, Benzidine-based Schiff base compounds for employing as corrosion inhibitors for carbon steel in 1.0 M HCl aqueous media by chemical, electrochemical and computational methods, *Journal of Molecular Liquids*, **317**(2020) 114015

[10] A. R. H. Zadeh, I. Danaee, M. H. Maddahy, Thermodynamic and adsorption behaviour of medicinal nitramine as a corrosion inhibitor for AISI steel alloy in HCl solution, *Journal of Materials Science & Technology*, **29**(2013) 884-892.

[11] A. Popova, M. Christov, A. Vasilev, Mono- and dicationic benzothiazolic quaternary ammonium bromides as mild steel corrosion inhibitors. Part II: Electrochemical impedance and polarisation resistance results, *Corrosion Science*, **53** (2011) 1770–1777

[12] N. A. Negm, M. A. Migahed, R. K. Farag**,** A. A. Fadda, M. K. Awad, M. M. Shaban, High performance corrosion inhibition of novel tricationic surfactants on carbon steel in formation water: Electrochemical and computational evaluations, *Journal of Molecular Liquids*, **262** (2018) 363-375.

[13] I.B. Obot, D.D. Macdonald, Z.M. Gasem, Density functional theory (DFT) as a powerful tool for designing new organic corrosion

inhibitors. Part 1: an overview, *Corrosion Science*, **99** (2015) 1–30.

[14] S. Cao, D. Liu, H. Ding, J. Wang, H. Lu, J. Gui, Task-specific ionic liquids as corrosion inhibitors on carbon steel in 0.5 M HCl solution: An experimental and theoretical study, *Corrosion Science*, **153** (2019) 301–313

[15] M. A. Migahed, A. M. Al-Sabagh, E. A. Khamis, E. G. Zaki, Quantum chemical calculations, synthesis and corrosion inhibition efficiency of ethoxylated-[2-(2-{2-[2-(2-benzenesulfonylamino-ethylamino)-ethylamino]-ethylamino}-ethylamino)-ethyl]-4-alkyl-benzenesulfonamide on API X65 steel surface under H2S environment, *Journal of Molecular Liquids*, **212** (2015) 360-371.

[16] Y. Qiang, S. Zhang, & L. Wang, Understanding the adsorption and anticorrosive mechanism of DNA inhibitor for copper in sulfuric acid, *Applied Surface Science*, **492** (2019) 228-238.

[17] M. A. Ismail, M. M. Shaban, E. Abdel-Latif, F. H Abdelhamed, M. A Migahed, M. N El-Haddad, A. S. Abousalem, Novel cationic aryl bithiophene/terthiophene derivatives as corrosion inhibitors by chemical, electrochemical and surface investigations, *Scientific Reports*, **12** (2022) 3192

[18] I. Ahamad, R. Prasad, M. A. Quraishi, Adsorption and inhibitive properties of some new Mannich bases of Isatin derivatives on corrosion of mild steel in acidic media, *Corros. Sci.*, **52** (2010) 1472-1481.

[19] M. A. Migahed, M. M. Shaban, A. A. Fadda, T. A. Ali, N. A. Negm, Synthesis of some quaternary ammonium gemini surfactants and evaluation of their performance as corrosion inhibitors for carbon steel in oil well formation water containing sulfide ions, *RSC Advances*, **5** (2015) 104480–104492

[20] Y. S. Choi, S. Nesic, S. Ling, Effect of H_2S on the CO_2 corrosion of carbon steel in acidic solutions, *Electrochimica Acta*, *56*(2011), 1752-1760.

[21] F. Pessu, R. Barker, & A. Neville, Pitting and uniform corrosion of X65 carbon steel in sour corrosion environments: the influence of CO_2, H_2S, and temperature. *Corrosion*, *73*(2017), 1168-1183.

[22] M. A. Migahed, A. M. Al-Sabagh, E. G. Zaki, H. A. Mostafa, A. S. Fouda, Synthesis of Some Novel Cationic Surfactants and Evaluation of Their Performance as Corrosion Inhibitors for X-65 type Carbon Steel under H_2S Environment, *International Journal of Electrochemical Science*, **9**(2014) 7693–7711

[23] I.B. Obota, M.M. Solomon, S.A. Umoren, R. Suleiman, M. Elanany, N.M. Alanazi, A. A. Sorour, Progress in the development of sour corrosion inhibitors: Past, present, and future perspectives, *Journal of Industrial and Engineering Chemistry*, **79** (2019) 1–18

[24] M. A. Moselhy, E. G. Zaki, S. A. Abd El-Maksoud, M. A. Migahed, Surface Activity and Electrochemical Behavior of Some Thiazine Cationic Surfactants and Their Efficiency as Corrosion Inhibitors for Carbon Steel in a Sour Environment, *ACS omega*, **6** (2021) 19559-19568.

[25] Y. El Mendili, A. Abdelouas, J. F. Bardeau, The corrosion behavior of carbon steel in sulfide aqueous media at 30°C, *Journal of materials engineering and performance*, **23**(2014) 1350-1357.

[26] M. A. Migahed, N. A. Negm, M. M. Shaban, T. A. Ali and A. A. Fadda, Synthesis, Characterization, Surface and Biological Activity of Diquaternary Cationic Surfactants Containing Ester Linkage, *Journal of Surfactants and Detergents*, **19**(2016) 119–128.

[27] ASTM G3-89, Standard practice for conventions applicable to electrochemical measurements in corrosion testing, 1994.

[28] M. Mobin, R. Aslam, R. Salim, S. Kaya, An investigation on the synthesis, characterization and anti-corrosion properties of choline based ionic liquids as novel and environmentally friendly inhibitors for mild steel corrosion in 5% HCl, *Journal of Colloid and Interface Science*, **620** (2022) 293–312

[29] R. Hsissou, S. Abbout, F. Benhiba, R. Seghiri, Z. Safi, S. Kaya, S. Briche, G. Serdarogˇlu, H. Erramli, A. Elbachiri, A. Zarrouk, A. El Harfi, Insight into the corrosion inhibition of novel macromolecular epoxy resin as highly efficient inhibitor for carbon steel in acidic mediums: Synthesis, characterization, electrochemical techniques, AFM/UV–Visible and computational investigations, *Journal of Molecular Liquids*, **337** (2021) 116492

[30] A. Chaouiki, H. Lgaz, I. M. Chung,, I. H. Ali, S. L. Gaonkar, K. S. Bhat, R. Salghi, H. Oudda, M. I. Khan, Understanding corrosion inhibition of mild steel in acid medium by new benzonitriles: insights from experimental and computational studies. *Journal of Molecular Liquids*, **266**(2018)603-616.

[31] Ahmed A. Farag, A.M. Eid, Mahmoud M. Shaban, Eslam A. Mohamed, Gunasunderi Raju, Integrated modeling, surface, electrochemical and biocidal investigations of novel benzothiazoles as corrosion inhibitors for shale formation well stimulation, *Journal of Molecular Liquids*, **336** (2021) 116315

[32] J. Saranya, F. Benhiba, N. Anusuya, R. Subbiah, A. Zarrouk, S. Chitra, Experimental and computational approaches on the pyran derivatives for acid corrosion, *Colloids and Surfaces A: Physicochemical and Engineering Aspects*, **603**(2020) 125231.

[33] E. H. El Tamany, S. M. Elsaeed, H. Ashour, E. G. Zaki, H. A. El Nagy, Novel acrylamide ionic liquids as anti-corrosion for X-65 steel dissolution in acid medium: Adsorption, hydrogen evolution and mechanism, *Journal of Molecular Structure*, **1168**(2018)106-114.

[34] M. Chafiq, A. Chaouiki, M. Damej, H. Lgaz, R. Salghi,, I. H. Ali, M. Benmessaoud, S. Masroor, Chung, I. M. Bolaamphiphile-class surfactants as corrosion inhibitor model compounds against acid corrosion of mild steel. *Journal of Molecular Liquids*, **309** (2020)113070.

[35] C. Verma, A. A. Sorour, E. E. Ebenso, M. A. & Quraishi, Inhibition performance of three naphthyridine derivatives for mild steel corrosion in 1M HCl: Computation and experimental analyses, *Results in Physics*, **10**(2018) 504-511.

[36] M. M. Shaban, N. A. Negm, R. K. Farag, A. A. Fadda, A. E. Gomaa A. A. Farag M. A. Migahed, " Anti-corrosion, antiscalant and anti-microbial performance of some synthesized trimeric cationic imidazolium salts in oilfield applications", *Journal of Molecular Liquids*, **351**(2022) 118610

[37] W. Zhuang, X. Wang, W. Zhu, Y. Zhang, D. Sun, R. Zhang, C. Wu, Imidazoline Gemini surfactants as corrosion inhibitors for carbon steel X70 in NaCl solution. *ACS omega*, **6**(2021), 5653-5660.

[38] M. N. El-Din, R. K. Farag, O. E. Elazbawy, Utilization of new anionic polymeric surfactants for corrosion inhibition enhancement in petroleum industries, *International Journal of Electrochemical Science*, **11**(2016) 815-835.

[39] E. M. S. Azzam, M. A. Hegazy, N. G. Kandil, A. M. Badawi, R. M. Sami, The performance of hydrophobic and hydrophilic moieties in synthesized thiol cationic surfactants on corrosion inhibition of carbon steel in HCl. *Egyptian journal of petroleum*, **24**(2015), 493-503.

[40] M. M. Shaban, A. M. Eid R. K. Farag, N. A. Negm, A. A. Fadda, M. A. Migahed, Novel trimeric cationic pyrdinium surfactants as bi-functional corrosion inhibitors and antiscalants for API 5L X70 carbon steel against oilfield formation water, *Journal of Molecular Liquids*, **305** (2020) 112817

[41] S. S. Durodola, A. S. Adekunle, L. O. Olasunkanmi, J. A. Oyekunle, Inhibition of mild steel corrosion in acidic medium by extract of Spilanthes uliginosa leaves, *Electroanalysis*, **32**(2020), 2693-2702.

[42] R. T. Loto, C. A. Loto, O. Joseph, G. Olanrewaju, Adsorption and corrosion inhibition properties of thiocarbanilide on the electrochemical behavior of high carbon steel in dilute acid solutions, *Results in Physics*, **6**(2016) 305-314.

[43] M. A. Moselhy, E. G. Zaki, S. A. E. H. Abd El-Maksoud, M. A. Migahed, The Role of Some Cationic Surfactants Based on Thiazine as Corrosion Inhibitors in Petroleum Applications: Experimental and Theoretical Approach, *ACS omega*,**7** (2022) 32014–32025

[44] A. Singh, Y. Caihong, Y. Yaocheng, N. Soni, Y. Wu, Y. Lin, Analyses of new electrochemical techniques to study the behavior of some corrosion mitigating polymers on N80 tubing steel, *ACS Omega*, **4**(2019) 3420-3431.

[45] X. Zhang, M. Zhang, Z. Zhang, Q. Li, R. Lv, W. Wu, Bis-Mannich bases as effective corrosion inhibitors for N80 steel in 15% HCl medium, *Journal of Molecular Liquids*, **347** (2022) 117957

[46] S. Satpati, A. Suhasaria, S. Ghosal, A. Saha, S. Dey, D. Sukul, Amino acid and cinnamaldehyde conjugated Schiff bases as proficient corrosion inhibitors for mild steel in 1 M HCl at higher temperature and prolonged

exposure: Detailed electrochemical, adsorption and theoretical study, *Journal of Molecular Liquids*, **324** (2021) 115077

[47]] K. Cherrak, O. M. A. Khamaysa, H. Bidi, M. El Massaoudi, Ismat A. Ali, S. Radi, Y. El Ouadi, F. El-Hajjaji, A. Zarrouk, and A. Dafali, Performance evaluation of newly synthetized bi-pyrazole derivatives as corrosion inhibitors for mild steel in acid environment, *Journal of Molecular Structure* **1261** (2022)132925.

[48] A. Y. Yassin , A. M. Abdelghany M. M. Shaban, Y. M. Abdallah, Synthesis, characterization and electrochemical behavior for API 5L X70 carbon steel in 5% sulfamic acid medium using PVVH/PEMA blend filled with gold nanoparticles, *Colloids and Surfaces A: Physicochemical and Engineering Aspects*, **635**(2022)128115

[49] A. Döner, R. Solmaz, M. Özcan, G. Kardas, Experimental and theoretical studies of thiazoles as corrosion inhibitors for mild steel in sulphuric acid solution, *Corrosion Science*, **53** (2011) 2902–2913

[50] H. H. Zhang, Y. Chen, Experimental and theoretical studies of benzaldehyde thiosemicarbazone derivatives as corrosion inhibitors for mild steel in acid media, *Journal of Molecular Structure*, **1177** (2019) 90-100

[51] P. Dohare,, K. R. Ansari, M. A. Quraishi, I. B. Obot, Pyranpyrazole derivatives as novel corrosion inhibitors for mild steel useful for industrial pickling process: experimental and quantum chemical study. *Journal of industrial and engineering chemistry*, 52 (2017)197-210

[52] S. M. Elsaeed, H. El Sayed, H. Ashour, E. G. Zaki, E. A. Khamis, H. A. El Nagy, Corrosion and hydrogen evolution rate control for X-65 carbon steel based on chitosan polymeric ionic liquids: experimental and quantum chemical studies. *RSC advances*, ***8***(2018)37891-37904.

[53] H. M. Abd El-Lateef, , A. M. Abu-Dief, M. A. Mohamed, Corrosion inhibition of carbon steel pipelines by some novel Schiff base compounds during acidizing treatment of oil wells studied by electrochemical and quantum chemical methods, *Journal of Molecular Structure*, **1130**(2017) 522-542.

[54] A. El-Aal, M. Sliem, A. Abdullah, Caprylamidopropyl Betaine as a highly efficient eco-friendly corrosion inhibitor for API X120 steel in 1 M H_2SO_4, *Egyptian Journal of Chemistry*, **63**(2020), 759-776.

[55] Ahmed H. Tantawy, Mahmoud M. Shaban, Hong Jiang, Man-Qun Wang, Hany I. Mohamed, Construction, petro-collecting/dispersing capacities, antimicrobial activity, and molecular docking study of new cationic surfactant-sulfonamide conjugates, *Journal of Molecular Liquids*, **334** (2021) 116068

[56] P. Kannan, A. Varghes, K., Palanisamy, & A. S. Abousalem, Evaluating prolonged corrosion inhibition performance of benzyltributylammonium tetrachloroaluminate ionic liquid using electrochemical analysis and Monte Carlo simulation, *Journal of Molecular Liquid*s, **297**(2020) 111855.

[57] L. H. Madkour, S. Kaya, & I. B. Obot, Computational, Monte Carlo simulation and experimental studies of some arylazotriazoles (AATR) and their copper complexes in corrosion inhibition process, *Journal of Molecular Liquids*, **260** (2018) 351-374.

[58] Farag, A. A., Abdallah, H. E., Badr, E. A., Mohamed, E. A., Ali, A. I., & El-Etre, A. Y. (2021). The inhibition performance of morpholinium derivatives on corrosion behavior of carbon steel in the acidized formation water: Theoretical, experimental and biocidal evaluations. Journal of Molecular Liquids, 341, 117348.

[59] Hashem, H. E., Farag, A. A., Mohamed, E. A., & Azmy, E. M. (2022). Experimental and theoretical assessment of benzopyran compounds as inhibitors to steel corrosion in aggressive acid solution. Journal of Molecular Structure, 1249, 131641.

[60] Mohamed, E. A., Hashem, H. E., Azmy, E. M., Negm, N. A., & Farag, A. A. (2021). Synthesis, structural analysis, and inhibition approach of novel eco-friendly chalcone derivatives on API X65 steel corrosion in acidic media assessment with DFT & MD studies. Environmental Technology & Innovation, 24, 101966.

[61] Farag, A. A., Eid, A. M., Shaban, M. M., Mohamed, E. A., & Raju, G. (2021). Integrated modeling, surface, electrochemical, and biocidal investigations of novel benzothiazoles as corrosion inhibitors for shale formation well stimulation. Journal of Molecular Liquids, 336, 116315.

[62] Osman, M. M., El-Ghazawy, R. A., & Al-Sabagh, A. M. (2003). Corrosion inhibitor of some surfactants derived from maleic-oleic acid adduct on mild steel in 1 M H2SO4. Materials chemistry and physics, 80(1), 55-62.

[63] Al-Neami, K. K., Mohamed, A. K., Kenawy, I. M., & Fouda, A. S. (1995). Inhibition of the corrosion of iron by oxygen and nitrogen containing compounds. Monatshefte für Chemie/Chemical Monthly, 126(4), 369-376.